Electronic Supplementary Material (ESI) for RSC Advances.

Supplementary information

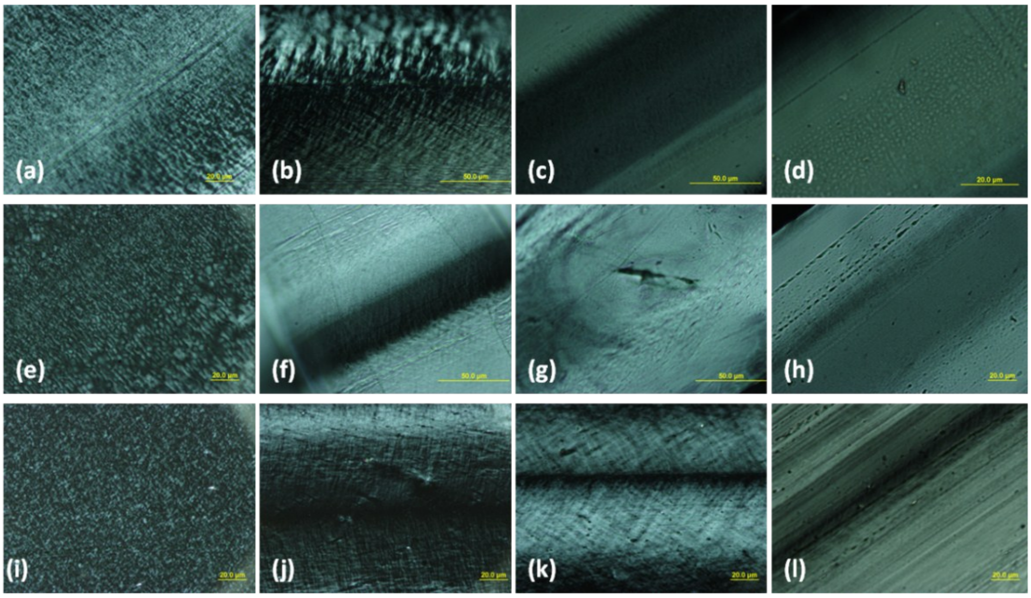

Figure S1. Representative POM images of OBC films: (a).OBC-35-DR3; (b). OBC-35-DR4.95; (c). OBC-35-DR8; (d). OBC-35-DR13.2; (e). OBC-25-DR3; (f). OBC-25-DR4.95; (g). OBC-25-DR8; (h). OBC-12-DR13.2; (j). OBC-12-DR3; (k). OBC-12-DR4.95; (I). OBC-12-DR8; (l). OBC-12-DR13.2. Note: The images were collected along the melt stretching direction.

In order to demonstrate the effect of melt stretching on crystal structure, the morphologies of OBC films with various DRs were firstly characterized by POM. Figure S1 shows several representative POM images for OBC films with different draw ratios. Due to the temperature gradient during cooling, all the films generally achieve skin-core structure and the core structure is the main component and dominates the final property of the films. Hence, we mainly focus on the core structures. For unoriented films, the spherulites are closely packed with a clear boundary. Figures S1a, S1e, S1i show clear spherulites for samples with DR3. The spherulite size for OBC-12 is also smaller than that of OBC-25 and OBC-35. After melt stretching, the spherulite size for all OBCs decreases significantly. With further increasing the draw ratio, the crystal size gradually decreases along the stretching direction.

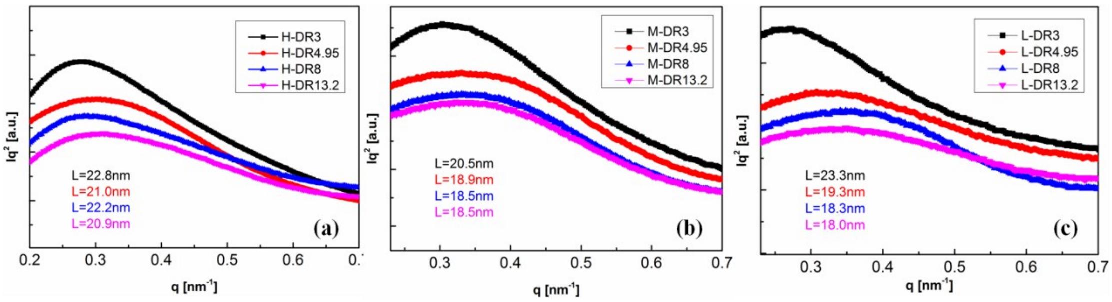

Figure S2. Lorentz-corrected 1d-SAXS curves and related long period (L) of (a). OBC-35; (b). OBC-25; (c). OBC-12 films with different draw ratios.

Figure S2 presents the Lorentz-corrected 1d-SAXS profiles for three OBCs with various draw ratios. After the Lorenz correction, a scattering peak from the lamellar structure can be seen from the curves. The peak locations gradually shift to the high-q zone. The long period L can be thus calculated by

$$L=2\pi/q_{max}, \quad (1)$$

where q_{max} is the scattering vector at the peak position of the 1d-SAXS curves. For all OBC films, long period gradually decreases with the increase in the draw ratio. The difference of long period between high DR and low DR for OBC-35, OBC-25 and OBC-12 are about 1.9±0.2nm, 2.0±0.2nm and 5.3±0.2nm, respectively. The decreased long period can mainly be attributed to the fragmented crystals or tiny crystals forming in samples with high draw ratio. The amorphous chains may orient/relax along the stretching direction but the distance between tiny crystals dominates the final long period. Long period can give information on the distribution of lamellae in amorphous network. In some other systems, it was found that the melt draw ratio are sensitive to change the lamellar lateral size but insensitive to change the long period or lamellar thickness[1].

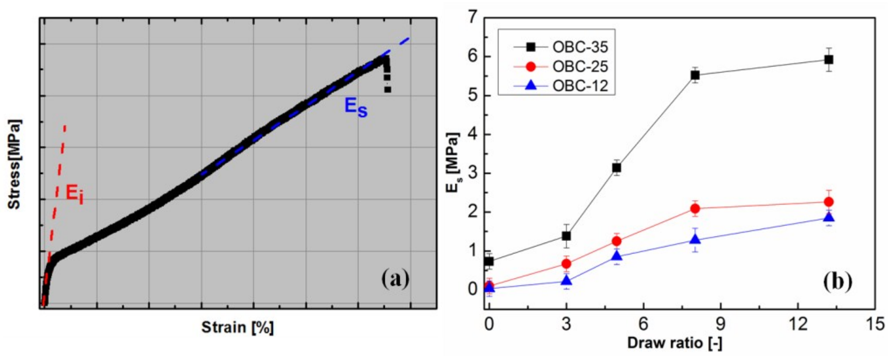

Figure S3. Schematic profiles for structures of OBC films: (a). typical stress-strain for initial modulus(E_i) and strain hardening modulus(E_s); (b). the strain-hardening modulus E_s as a function of draw ratio.

Furthermore, the strain hardening behaviors of these films were discussed in detail. Based on the discussion of Strobl, during tensile testing of polyethylene, a further increase in the true strain can result in better fibril alignment and can give rise to strong strain hardening [2]. This interpretation seems to be appropriate for our samples. Figure S3a presents different stages during deformation and shows two modulus including initial Young's modulus (E_i) and strain hardening modulus (E_s). In our system, the fibril (shish) structure may dominate the strain hardening behavior. This phenomenon can be similar with the case in the fiber-reinforced composites [3-4]. Well stress-transfer of fibrils induces high mechanical performance at large deformation especially during strain hardening process. As shown in Figure S3b, the strain hardening modulus (E_s) slightly increases for OBC-25 and OBC-12 while it increase significantly for OBC-35, which is strongly similar with the increasing trend of shish content. Again, the rigid crystalline network in OBC-35 is destructed at high draw ratio and thus leading to high shish content with well alignment, which are in great favor of strain hardening modulus.

References

1. R. Xu, X. Chen, J. Xie, Q. Cai and C. Lei, *Ind. Eng. Chem. Res.*, 2015, **54**, 2991.
2. M. Al-Hussein and G. Strobl, *Macromolecules*, 2002, **35**, 8515.
3. Z. Wang, Y. Niu, G. H. Fredrickson, E. J. Kramer, Y.-W. Shin, F. Shimizu, F. Zuo, L. Rong, B. S. Hsiao and G. W. Coates, *Macromolecules*, 2010, **43**, 6782.
4. M. Hietala, E. Samuelsson, J. Niinimäki and K. Oksman, *Composites Part A: Appl. Sci.,* 2011, **42**, 2110.